Infection and Drug Resistance

Dovepress
Taylor & Francis Group

Open Access Full Text Article

ORIGINAL RESEARCH

Mass Cytometry Analysis of High-Dimensional Single-Cell Immune Profiles in ZF2001-Vaccinated Patients Infected with SARS-CoV-2

Xin Zhang[1,2,*], Li Li[3,4,*], Yongmei Liu[5,*], Haoting Zhan[5,*], Muwei Dai[6], Kun Zhang[7], Huimin Yan[8], Huixia Gao[9], Jingwen Liu[10], Shifu Liu[2], Weina Lu[7], Yongzhe Li[5], Aidong Feng[7], Erhei Dai[3,9], Junying Zhou[1]

[1]Department of Infectious Disease, The Third Hospital of Hebei Medical University, Shijiazhuang, Hebei, People's Republic of China; [2]Department of Tuberculosis, The Fifth Hospital of Shijiazhuang, Hebei Medical University, Shijiazhuang, Hebei, People's Republic of China; [3]Department of Internal Medicine, Hebei Medical University, Shijiazhuang, Hebei, People's Republic of China; [4]Intensive Care Unit, The Fifth Hospital of Shijiazhuang, Hebei Medical University, Shijiazhuang, Hebei, People's Republic of China; [5]Department of Clinical Laboratory, State Key Laboratory of Complex, Severe and Rare Diseases, Peking Union Medical College Hospital, Chinese Academy of Medical Science and Peking Union Medical College, Beijing, People's Republic of China; [6]Department of Orthopedics, The Fourth Hospital of Hebei Medical University and Hebei Cancer Hospital, Shijiazhuang, Hebei, People's Republic of China; [7]Department of Infectious Diseases, The Fifth Hospital of Shijiazhuang, Hebei Medical University, Shijiazhuang, Hebei, People's Republic of China; [8]Clinical Research Center, The Fifth Hospital of Shijiazhuang, Hebei Medical University, Shijiazhuang, Hebei, People's Republic of China; [9]Department of Laboratory Medicine, The Fifth Hospital of Shijiazhuang, Hebei Medical University, Shijiazhuang, Hebei, People's Republic of China; [10]Department of Infectious Diseases, Baoding First Central Hospital, Baoding, Hebei, People's Republic of China

*These authors contributed equally to this work

Correspondence: Erhei Dai; Junying Zhou, Email daieh2008@126.com; doctorzhoujy@163.com

Introduction: Coronavirus disease 2019 (COVID-19), caused by the severe acute respiratory syndrome coronavirus 2 (SARS-CoV-2), was declared a public health emergency of international concern (PHEIC) by the WHO. ZF2001, a protein subunit vaccine targeting the RBD, was utilized to evaluate its impact on the immune system of COVID-19 patients. This study aimed to investigate peripheral cell profiles one year after three doses of ZF2001 vaccine using single cell mass spectrometry flow cytometry (CyTOF), a technique that allows detailed characterization of the immune response against SARS-COV-2 infection and further evaluation of ZF2001 mechanisms as a prophylactic against chronic disease and reducing mortality.

Methods: This study profiled peripheral blood mononuclear cells (PBMCs) from 16 vaccinated COVID-19 patients (Omicron 5.2) and 8 hDs using CyTOF with a 41-antibody panel. PBMCs isolated via Lymphoprep density gradient underwent metal-tagged antibody staining. Data analysis included FlowJo gating, Seurat/Harmony batch correction, PhenoGraph clustering (k=45), and t-SNE visualization. Statistical assessments employed Wilcoxon tests and Spearman correlation.

Results: Our findings revealed significant differences between infected and healthy individuals one year after three doses of ZF2001. Specifically, infected individuals exhibited: significant elevation of cytotoxic T cells expressing CD8 with a proliferation marker antigen-Kiel 67 (Ki67) and an adhesion molecule (CD138), expansion of B cells and reduction of monocytes expressing CD16, as well as depletion of CD4+ T cells and differentiation of T cells 1 year after the vaccine. These changes suggested that the vaccine was effectively modulating the immune response.

Discussion: Our results provided a detailed single-cell profile of the immune response to SARS-CoV-2 infection in vaccinated patients, highlighting significant changes in immune cell kinetics indicative of an active innate and adaptive immune cell response.

Keywords: COVID-19, vaccine, ZF2001, CyTOF, immune response

Introduction

The risk of infection as well as acute or chronic COVID-19 disease manifestation, caused by severe acute respiratory syndrome coronavirus (SARS-CoV-2), a variety of variants continue to evolve and circulate (eg, BA1, BQ1, JN1) with current variants denoted as XEC and KP3.1.1.[1,2] Vaccination plays a key role in establishing an immunity barrier against

Received: 12 December 2024
Accepted: 5 May 2025
Published: 14 May 2025

© 2025 Zhang et al. This work is published and licensed by Dove Medical Press Limited. The full terms of this license are available at https://www.dovepress.com/terms.php and incorporate the Creative Commons Attribution – Non Commercial (unported, v4.0) License (http://creativecommons.org/licenses/by-nc/4.0/). By accessing the work you hereby accept the Terms. Non-commercial uses of the work are permitted without any further permission from Dove Medical Press Limited, provided the work is properly attributed. For permission for commercial use of this work, please see paragraphs 4.2 and 5 of our Terms (https://www.dovepress.com/terms.php).

COVID-19 by stimulating the innate and adaptive immune systems against SARS-CoV-2,[3] together with stimulating antibody production by the host.[4] Evidence has already proved to be effective in reducing the rates of death, severity of illness, and, to some extent, household transmission.[4–6] Moreover, the overall risk reduction (ORR) probably is around 86% of serious disease and mortality although efficacy remains subjective.[7]

ZF2001 is a protein subunit vaccine that uses a tandem-repeat SARS-CoV-2 spike receptor-binding domain (RBD) dimer as the antigen.[8] ZF2001 was shown to be safe and effective in a Phase 3 clinical trial (ClinicalTrials.gov number, NCT04646590) conducted at 31 clinical sites in Uzbekistan, Indonesia, Pakistan and Ecuador.[9] ZF2001 received emergency use authorization in both China and Uzbekistan in March 2021, and is being administered through a three-dose vaccination regimen.[8] A proteomics study has shown that people vaccinated with ZF2001 have elevated expression of Immunoglobulin Kappa Variable(IGKV), Immunoglobulin Heavy Variable (IGHV), interleukin-17 (IL-17) signaling, and the phagocytosis pathway, along with lower expression of Fibrinogen-like protein 2 (FGL2) compared to the non-vaccinated group which indicated high immune response.[10] However, we lack information on the changes in the immune profile at the single-cell level for the ZF2001 vaccinated group when they are infected by SARS-CoV-2.

However, to the best of our knowledge, no research has investigated the changes in the immune cell microenvironment of ZF2001 vaccinated patients during the post-infection period. Mass cytometry, also called Time of Flight (CyTOF), is a powerful and suitable tool for high-dimensional and high-throughput single-cell assays to interrogation changes in the immune microenvironment.[11] By incubation live cells with metal isotopes labeled antibodies, time of flight mass spectrometry from CyTOF could recognize various antibodies by detecting isotopes they carry.[12] Single cell screening were achieved by nebulizing suspensions so that each droplet encapsulated just one cell.[11] These individual cells were then directed through an argon (Ar) plasma, which served to atomize and ionize the cells.[11] As a result, each cell was transformed into a cloud of ions representing the elements found within or on the surface of the cell. By combining single cell screening and mass spectrometry techniques, CyTOF could screen up 40 antibodies for a single cell in practice.[11]

CyTOF enables the simultaneous analysis of chemokines and their receptors, such as CXCR3 and CCR4, across multiple cell types in a single experiment. CXCR3 is key in inflammatory responses against viral infections, while CCR4 is essential for T-cell lung imprinting.[13,14] Past CyTOF studies have revealed $CD4^+$ T-cell depletion, T-cell differentiation, plasma cell expansion, and reduced antigen presentation capacity of innate immune cell phenotypes in the context of COVID-19 which are MHC type I and MHC type II (or HLA haplotypes).[12,15,16] The disease also induces a dysregulation in the balance of monocyte populations through the expansion of monocyte subsets.[15,17,18] Monocyte cell subsets potentially including expansion or differentiation of classical, non-classical and intermediate which could be affected by metabolic factors requiring further research.

Although ZF2001, a prophylactic COVID-19 vaccine, demonstrated 87.6% efficacy against severe disease in clinical trials,[9] there remains a paucity of data on the roles of innate and adaptive immunity at the single-cell level during the post-infection period. Therefore, we performed CyTOF on patients diagnosed with COVID-19 who had been pre-injected with three doses of ZF2001. In this study, the peripheral blood mononuclear cells were profiled by CyTOF for 16 patients and 8 health donors. Using automated clustering without supervision, we unveiled the PBMC landscape for vaccinated patients in responses to COVID-19.

Method

Patients and Data Collection

A total of 16 COVID-19 hospitalized patients were recruited for this study at the Fifth Hospital of Shijiazhuang, China, between October 15 and October 18, 2022. The target population comprised university students aged 18 to 21 years old who tested positive for corona virus nucleic acid detection kit (DaAnGene, Guangzhou, China) real-time reverse-transcriptase quantitative PCR (RT-gPCR). The patients were infected with the Omicron BA. 5.2 strain. Patients with negative SARS-CoV-2 tests or chronic underlying diseases were excluded from the study. Additionally, 8 healthy individuals were included as healthy donors (HDs) and served as controls (Supplementary Table 1). These HDs were close contacts of the COVID-19 patients (5 males, 3 females; mean age, 20 ± 0.5 years). All COVID-19 patients and HDs received the first dose of the ZF2001 vaccine on April 30, 2021, the second dose on June 8, 2021, and the third dose between July and September 2021. The patients contracted COVID-19 13 months post-vaccination, and blood samples

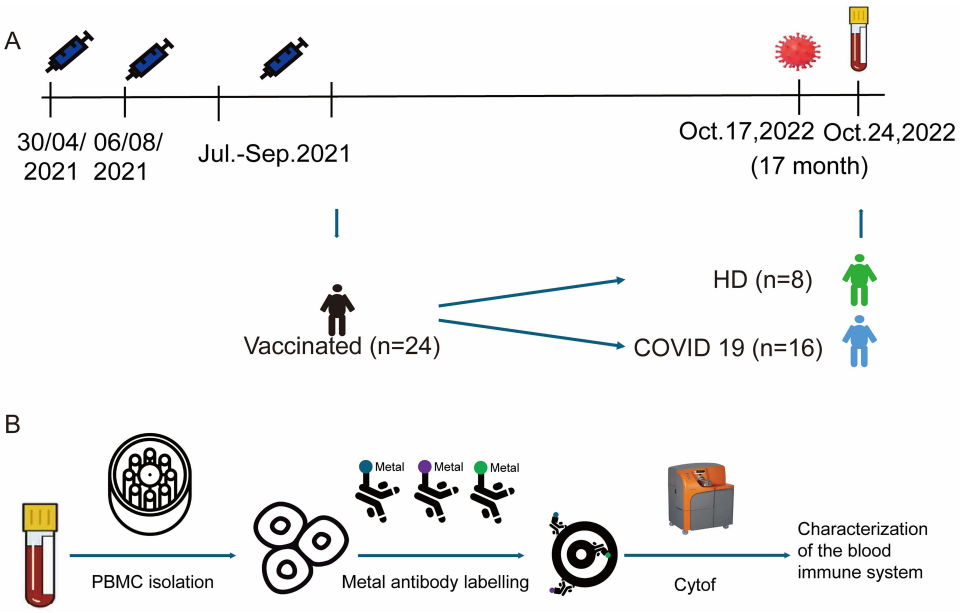

Figure 1 Timeline for vaccination, COVID-19 infection and sample acquisition followed by experimental approach. (**A**) Vaccination and sample collection schedule. The vaccination regimen with ZF2001 was administered in three doses. The first dose was administered over the course of one week, beginning on April 30, 2021. The second dose commenced on June 8, 2021, and was completed within two months. The third dose was administered between July and September 2021. A COVID-19 infection was recorded on October 17, 2022, followed by the collection of blood samples on October 24, 2022. In this study, 24 individuals were vaccinated, comprising 8 healthy controls and 16 COVID-19-infected participants. Infection of COVID19 had happened on Oct. 17, 2022 and blood sample were collected on Oct 24, 2022. In our study, 24 people were vaccinated. 8 of theme were health control (HD) and 16 were infected by COVID19. (**B**) Following isolation, peripheral blood mononuclear cells (PBMCs) were labeled with metal-tagged antibodies and analyzed using cytometry by time of flight (CyTOF) to assess immune responses.
Abbreviations: COVID-19, Coronavirus disease 2019; HD, health control; PBMCs, peripheral blood mononuclear cells; CyTOF, mass spectrometry flow cytometry.

were collected within one week of infection (Figure 1A). Participants were classified according to the Diagnosis and Treatment Protocol for Novel Coronavirus Pneumonia (Trial Version 7).[19] Mild cases were defined as patients with mild clinical symptoms and no signs of pneumonia on computed tomography (CT) scan imaging, while moderate cases presented with fever and respiratory symptoms, accompanied by imaging evidence of pneumonia. This cohort included 14 mild and 2 moderate cases (16 males; mean age, 20 ± 0.8 years).

Isolation of Peripheral Blood Mononuclear Cells (PBMCs)

Peripheral blood samples from the patients and healthy donors were processed using Lymphoprep™ (Stemcell Technologies). Each 5 mL blood sample was mixed with an equal volume of phosphate-buffered saline (PBS) and carefully layered over Lymphoprep™ density gradient medium in a tube, maintaining a ratio of 1:2 (density gradient medium to blood with phosphate-buffered saline), without mixing. The samples were then centrifuged at 1500 rpm for 10 minutes at 20°C. Peripheral blood mononuclear cells (PBMCs) were collected from the interface between the plasma and the density gradient medium. These cells were washed twice with FACS Buffer (1.25% bovine serum albumin in PBS) and centrifuged again at 1500 rpm for 5 minutes at 20°C. The PBMCs were then resuspended in FACS buffer. To prepare for cryopreservation, a freezing solution composed of 90% fetal bovine serum (FBS) and 10% dimethyl sulfoxide (DMSO) was added to the PBMCs. The cell concentration was adjusted to 5×10^6 cells/mL before storing in liquid nitrogen.

Metal Tagged Antibody Preparation and Staining for PBMCs

A panel of 41 antibodies used in our CyTOF analysis is detailed in Supplementary Table 1, including metal tag, clone, and provider information. Metal-labeled antibodies were prepared using the Maxpar X8 Antibody Labeling Kit (Standard Bio-Tools) following the manufacturer's instructions. After conjugation, the antibodies were diluted in Antibody Stabilizer PBS (Candor Bioscience) and stored long-term at 4 °C.

Frozen PBMCs were thawed in a 37 °C thermostatic water bath and then centrifuged at 1500 rpm for 5 minutes. Subsequently, the cells were resuspended in FACS Buffer. Around 200,000 cells per sample were used for antibody staining.

https://doi.org/10.2147/IDR.S511936

PBMCs were first stained with 50 nM Cisplatin (Fluidigm, San Francisco, CA) for 5 minutes to differentiate live and dead cells in future gating strategy. The cells were then washed with Cell Staining Buffer (Fluidigm) and centrifuged at 300 g for 5 minutes. Next, PBMCs were incubated with 50 µL of Fc receptor blocking solution (BioLegend, USA) at room temperature for 10 minutes. After blocking, 50 µL of the surface marker antibody cocktail was added to the PBMCs, followed by two washes with Cell Staining Buffer (CSB) at 300 g for 5 minutes each at room temperature. Cells were then fixed by adding 1 mL of 1X Maxpar Fix I Buffer and washed twice with 2 mL of Perm-S Buffer (Fluidigm) at 800 g for 5 minutes each at room temperature. Subsequently, cells were incubated with a cytoplasmic/secreted antibody cocktail (diluted 1:100, resulting in a final volume of 100 µL). Following this, cells were washed twice and incubated with Cell-ID Intercalator-Ir solution. The final concentration of the Ir intercalator was 0.125 nM diluted in 1.6% formaldehyde PBS. The sample was then washed with deionized water and resuspended at a concentration of $1.0*10^6$ cells/mL with the 1 in 10 dilution Eq.4 Element Beads solution (Fluidigm). Finally, the prepared samples were loaded onto a Helios (Fluidigm) system and acquired at a rate of 300–500 events per second to collect the raw data.

Mass Cytometry Data Analysis

The Fluidigm acquisition algorithm (V6.0.626) was employed to randomize the raw mass cytometry data. Individual samples were gated using FlowJo to exclude normalizing beads, cell debris, dead cells, and duplexes for further analysis to identify cells. Cell isolation was accomplished by configuring the x-axis to Event_length, adjusting the range to 0–60, and the y-axis to the EQ beads channel. Regions were selected where the x–values were below 40 and y-values were below 10^2 to remove EQ beads and isolate individual cells. To isolate live immune cells, the x-axis was set to CD45 and the y-axis to Pt platinum dye, typically selecting values around 10^2 or below on the y-axis and generally above 10^1 on the x-axis for live immune cells. The number of cells acquired by CyTOF and passing the above quality control procedure was summarized separately in Supplementary Table 3. Due to compactional resource limitation, data of 20,000 live $CD45^+$ cells from each sample were collected for further analysis.

Data were then transformed using asinh (cofactor 5) and normalized to the 99.9th percentile for each channel in the R environment (V3.6.1). For single-cell processing Seurat package in R, Harmony version 0.1.0 was utilized to mitigate batch effects. The *t*-test were performed by R 4.3.2. The picture was painted by ggplot2. Clustering was conducted using R phenograph version 0.99.1 with a specified parameter of "K=45". A heatmap was generated using Complex-Heatmap version 2.10.0 to exhibit the median z-score (ranging from 0 to 1) of marker expression across each cluster. T-distributed stochastic neighbor embedding (t-SNE) was employed for dimensionality reduction to explore the phenotypic diversity among cell populations.

Statistics

Given the heterogeneity of the clinical and CyTOF data, unpaired Wilcoxon tests were conducted throughout the study unless specified otherwise. The ggcorrplot R package facilitated Spearman's rank correlation analysis to identify phenotypically similar clusters. Significance levels were denoted as *P<0.05, **P<0.01, ***P<0.001, and ****P<0.0001.

Results

CyTOF Analysis of Peripheral Blood Mononuclear Cell Immune Profiles in COVID-19 Patients and Healthy Donors

A total of 24 participants, comprising 16 patients diagnosed with COVID-19 and 8 healthy donors (HD), were enrolled in this study. Their mean age was 20.38 ± 0.753 years with no underlying disease. 14 patients were diagnosed as mild while 2 were diagnosed as moderate. The information of all patients is summarized in Supplementary Table 1. All COVID-19 patients were male, and there were 3 females in HD. All participants had received three doses of the vaccine. The severity of the disease among the patients ranged from mild to moderate, as depicted in Figure 1A. To characterize the immune profiles of peripheral blood mononuclear cells (PBMCs), we employed cytometry by time of flight (CyTOF) due it could profile cell protein marker at single cell level. Samples were pooled and stained with a panel of heavy metal-conjugated antibodies, followed by acquisition on a mass cytometer (Figure 1B). Data processing was initiated using the Seurat package in R, where cells were classified into distinct phenotypes based on their marker expression and clustering

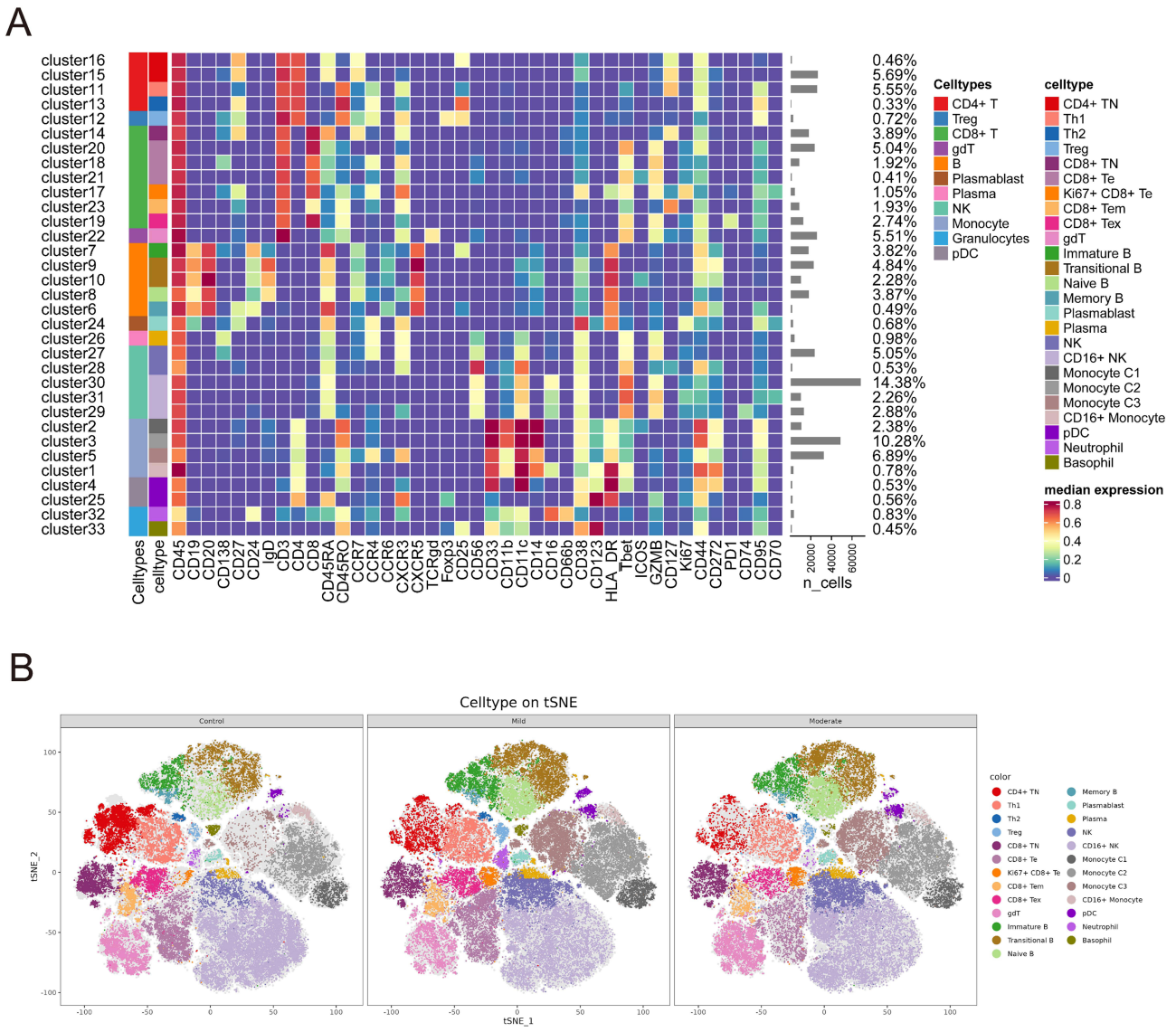

Figure 2 Peripheral blood mononuclear cell cluster sorting according to marker expression levels. (**A**) Heatmap of normalized immune cell marker expressing in 32 immune cell clusters. (**B**) T-stochastic neighbor embedding (T-SNE) map was colored by defined cell types in control, mild and moderated groups.

Abbreviations: T-SNE, T-stochastic neighbor embedding; T, T cells; B, B cells; Treg, regulatory T cells; gdT, gamma delta T cells; NK, natural killer cells; pDC, plasmacytoid dendritic cells; TN, naive T cells; Te, effector T cells; Tem, effector memory T cells; Tex, exhausted T cells; Th, helper T cells type I; Th2, helper T cells type 2; GZMB, Granzyme B; T-bet, T-box expressed in T cells; Foxp3, Forkhead box protein P3; ICOS, Inducible T-cell Costimulator; Ki67, Antigen identified by monoclonal antibody Ki-67; TCRgd, T Cell Receptor γδ; HLA-DR, Human Leukocyte Antigen-DR, PD1, Programmed cell death protein 1; IgD, Immunoglobulin D; CXCR3, C-X-C motif chemokine receptor 3; CXCR5, C-X-C motif chemokine receptor 5; CCR4, C-C Chemokine Receptor Type 4; CCR6, C-C Chemokine Receptor 6; CCR7, C-C Chemokine Receptor 7.

algorithms. $CD45^+$ immune cells were categorized into 33 subsets, as shown in Figure 2A. Differences in these subsets among mild, moderate and healthy donors are illustrated in Figure 2B. As The 32 cell clusters were categorized into seven lineages: 10 T cell subpopulations (we combined cluster18 cluster20 cluster 21 as one and cluster15 cluster16 as one), 4 B cell subpopulations (we combined cluster9 and cluster10 as one), 5 NK cell subpopulations, 4 monocyte subpopulations, 2 plasmacytoid dendritic cell (pDC) subpopulations, 1 neutrophil subpopulation, 1 basophil cell subpopulation and 1 plasma cell subpopulation. A comprehensive classification of $CD45^+$ immune cells, including the expression of key marker molecules, is provided in Supplementary Table 2 Due to only two samples were diagnosed as moderate, we combined moderate and mild data together as COVID 19 group for the following data analysis.

https://doi.org/10.2147/IDR.S511936

Increase of Ki67$^+$ CD8$^+$ Effector T Cells were Observed in COVID-19 Patients

The initiation of data analysis focused on T cells due to their roles in recognizing and destroying infected cells. Cells were divided into 10 T cell subtypes by t-SNE: naive T cells (TN, CD4+): CD45RA$^+$CCR7$^+$CD4$^+$, helper T cells type I (Th1): CD45RO$^+$ CXCR3$^+$ CD127$^+$ CD4$^+$, helper T cells type 2 (Th2): CD45RO$^+$ CD25$^+$ CCR4$^+$ CD27$^+$ CD4$^+$, regulatory T cells (Treg): CD45RO$^+$ CCR7 (low) CD27$^+$Foxp3$^+$CD25$^+$CCR4$^+$CXCR3$^+$ CD4$^+$, naive T cells (CD8$^+$ Tn): CD45RA$^+$CCR7$^+$CXCR3$^+$CD27$^+$CD127$^+$CD8$^+$, effector T cells (CD8$^+$ Te): CD45RA$^+$CCR4$^+$CXCR3$^+$ CD138^{low}GZMB$^+$CD8$^+$, T effector cells (Ki67$^+$CD8$^+$Te): Ki67$^+$ CD8$^+$, effector memory T cells (CD8$^+$ Tem): CD45RO$^+$CD127$^+$CXCR3$^+$CD8$^+$, exhausted T cells (CD8$^+$ Tex): CD45RO$^+$PD1$^+$GZMB$^+$CD8$^+$, and gamma delta T cells (gdT cells): TCRγδ$^+$CXCR3$^+$Tbet$^+$GZMB$^+$ (Figure 3A). Figure 3B illustrated the difference of COVID-19 and HD group on t-SNE. The total frequency of CD4$^+$ T cells were significantly higher in HD group due to there were more CD4$^+$ TN and Th2 cells (Figure 3C and D). Although there were no significant differences of the CD8$^+$ T cell frequency (Figure 3C). The Ki67$^+$CD8$^+$Te were significant higher in COVID-19 while CD8$^+$ Tem were higher in HD (Figure 3E). The gdT were also higher in HD while Treg were higher in COVID19 (Supplementary Figure 1A). To reveal the functional differences for T cells between COVID-19 and HD group, Wilcox test were used to perform differentiation analysis between COVID-19 and HD. $p<0.05$ and Log2FC>1 were the conditions to filter the data. The CCR4, CD138, and CXCR3 expressed cells were all significantly higher in COVID-19 T cells (Figure 3F and Supplementary Figure 1B). While CD44 expressed cells were all significantly lower in COVID 19 T cells (Figure 3G and Supplementary Figure 1B).

B Cells Elevated by COVID-19 Infection Play a Major Role in Humoral Immune Response

B cells are crucial for vaccinated related humoral immune response as they produce antibodies that provide long-lasting immunity against pathogens. 4 subtype of B cells were identified through t-SNE as CD25$^+$HLA_DR$^+$ CXCR5$^+$ CD24$^+$CD38^{low}immature B cells (immature B), CD24$^+$CD38$^+$lgD$^+$CCR7^{low}HLA_DR$^+$CXCR5$^+$ ICOS^{low} CD272$^+$transitional B cells (transitional B), CD24$^+$CD38^{low} lgD$^+$ CCR7$^+$ HLA_DR$^+$CXCR5$^+$ naïve B cells (naïve B) and CD27$^+$CD24$^+$CD45RA$^+$CCR6^{low}CXCR5$^+$HLA_DR$^+$memory B cells (memory B) (Figure 4A). Despite the memory B had no difference, the Naïve B, immature B and transitional B were all higher in COVID19 PBMC which indicated a strong positive humoral immune response from vaccinated patients (Figure 4B and C). The CXCR3 and CCR4 were higher in Naïve B, Memory B and immature B while CD27 were lower in memory B and immature B (Figure 4D). In the context of COVID-19, both CD19^{low}CD27^{high}CD38^{high}CCR4$^+$CXCR3$^+$HLA_DR$^+$Ki67$^+$plasmablasts (plasmablasts) and CD138$^+$CD38$^+$ CCR4$^+$CXCR3$^+$plasma cells (plasma cells), which are responsible for producing antibodies for short-term and long-term immunity, exhibited higher frequencies and expressed elevated levels of CXCR3 and CD138 in plasma cells, as well as CCR4 in plasmablasts. Conversely, there were lower levels of CD16 in plasma cells and reduced expression of CD27 and CD44 in plasmablasts (Supplementary Figure 2A and B). Our data suggested that in vaccinated patients, B cells proliferate and differentiate systemically in response to COVID-19 infection.

COVID-19 Induced Upregulation of Myeloid-Derived Cells and NK Cells in COVID PBMC

Myeloid-derived cells such as monocytes, neutrophil, and pDC play crucial roles in the immune system's antiviral response by phagocytosing pathogens, presenting antigens, producing cytokines, and forming extracellular traps to neutralize and eliminate viruses. Monocytes could be divided into 4 subtypes by t-SNE and they were monocyte C1, monocyte C2, monocyte C3 and CD16$^+$HLA_DR$^+$CD272$^+$CD16$^+$monocytes (CD16$^+$monocytes) in this research (Figure 5A). The monocyte C1 was defined as CD272$^+$CD95$^+$ICOS^{low} monocyte. The monocyte C2 was defined as CD272$^+$CD95$^+$monocyte. The monocyte C3 was defined as CCR4$^+$ CXCR3$^+$ CD272^{low} CD95$^+$ monocyte. The frequency of total monocytes was higher in COVID-19 patients. Specifically, monocyte subsets C2, and C3 were elevated (Figure 5B and C). Monocyte subset C3 in COVID-19 showed increased expression of CCR4, CCR7, CD11b, CD138, CD74, and CXCR3, while CD16$^+$ monocytes exhibited higher levels of CCR4, CD11b, CD138, CD38, CD4, CD45RO, CXCR3, and HLA-DR (Figure 5D). The frequency of neutrophils showed no difference, but they showed

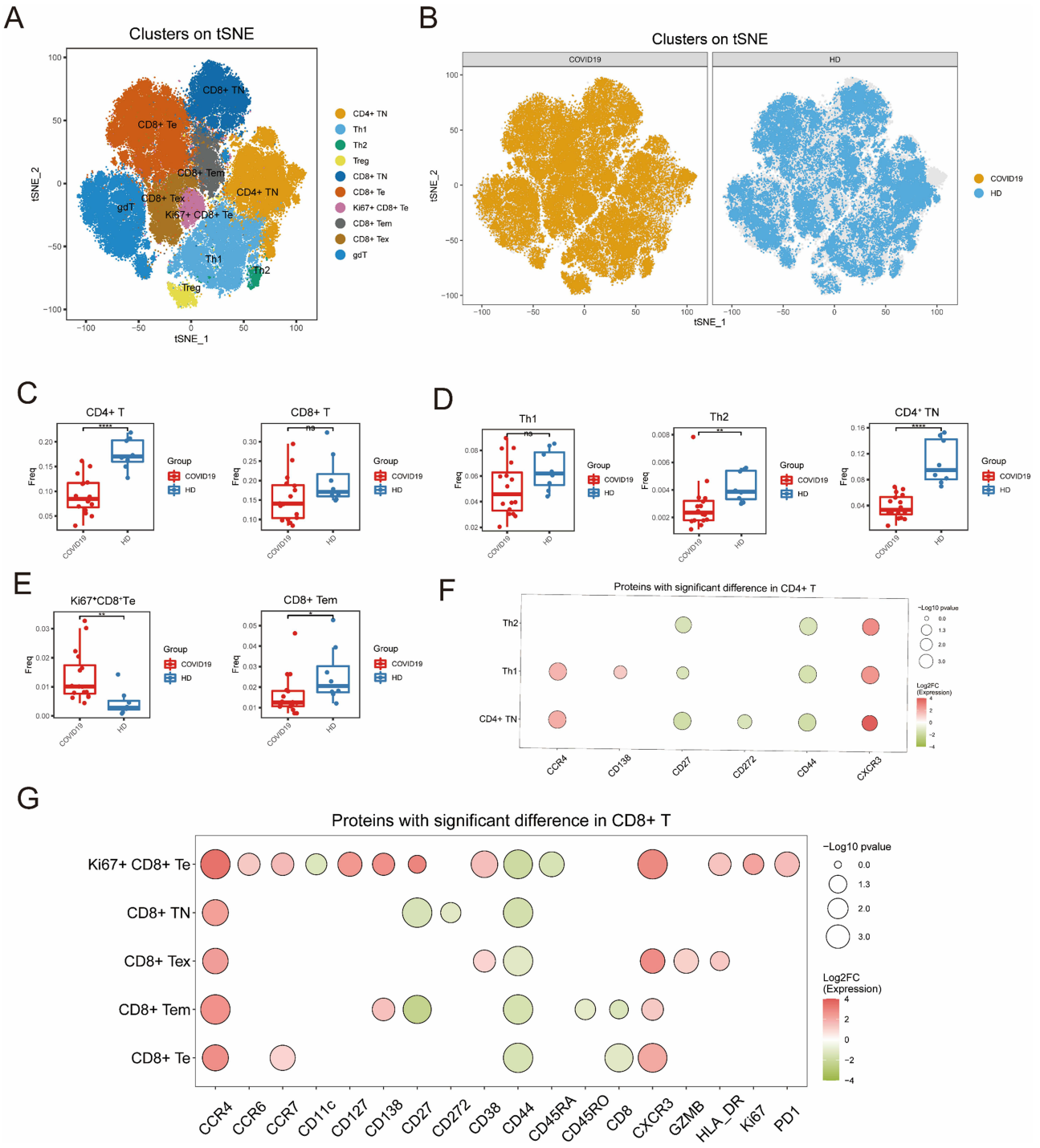

Figure 3 Comparative Analysis of T-cell Subsets in Healthy Donors and COVID-19 Patients. (**A**) t-Distributed Stochastic Neighbor Embedding (t-SNE) plot displaying the distribution of T-cell subsets, colored by cell type. (**B**) t-SNE projections illustrating major T-cell subsets in healthy donors and COVID-19 patients, colored by group. (**C**) Box plots depicting the frequency of $CD4^+$ T cells, which were significantly higher in healthy donors ($p<0.05$), while $CD8^+$ T cells showed no significant differences between the groups. (**D**) Box plots indicating reduced frequencies of Th1 cells, Th2 cells and $CD4^+$ T naive (TN) cells in COVID-19 patients compared to healthy donors. (**E**) Box plots showing an increased frequency of $Ki67^+CD8^+$ effector T cells (Te) in COVID-19 patients, whereas $CD8^+$ effector memory T cells (Tem) were lower. (**F**) Bubble plots illustrating proteins with significant differential expression in $CD4^+$ T cell subtypes between groups. (**G**) Bubble plots illustrating proteins with significant differential expression in $CD8^+$ T cell subtypes between groups. Dot size represents the negative log10 p-value, with green dots indicating higher expression in healthy donors and red dots indicating lower expression. Only proteins with an absolute log2 fold change over 1 and $p<0.05$ were selected for display following a unpaired Wilcoxon test. Significance levels were denoted as *P<0.05, **P<0.01, ***P<0.001, and ****P<0.0001.

https://doi.org/10.2147/IDR.S511936

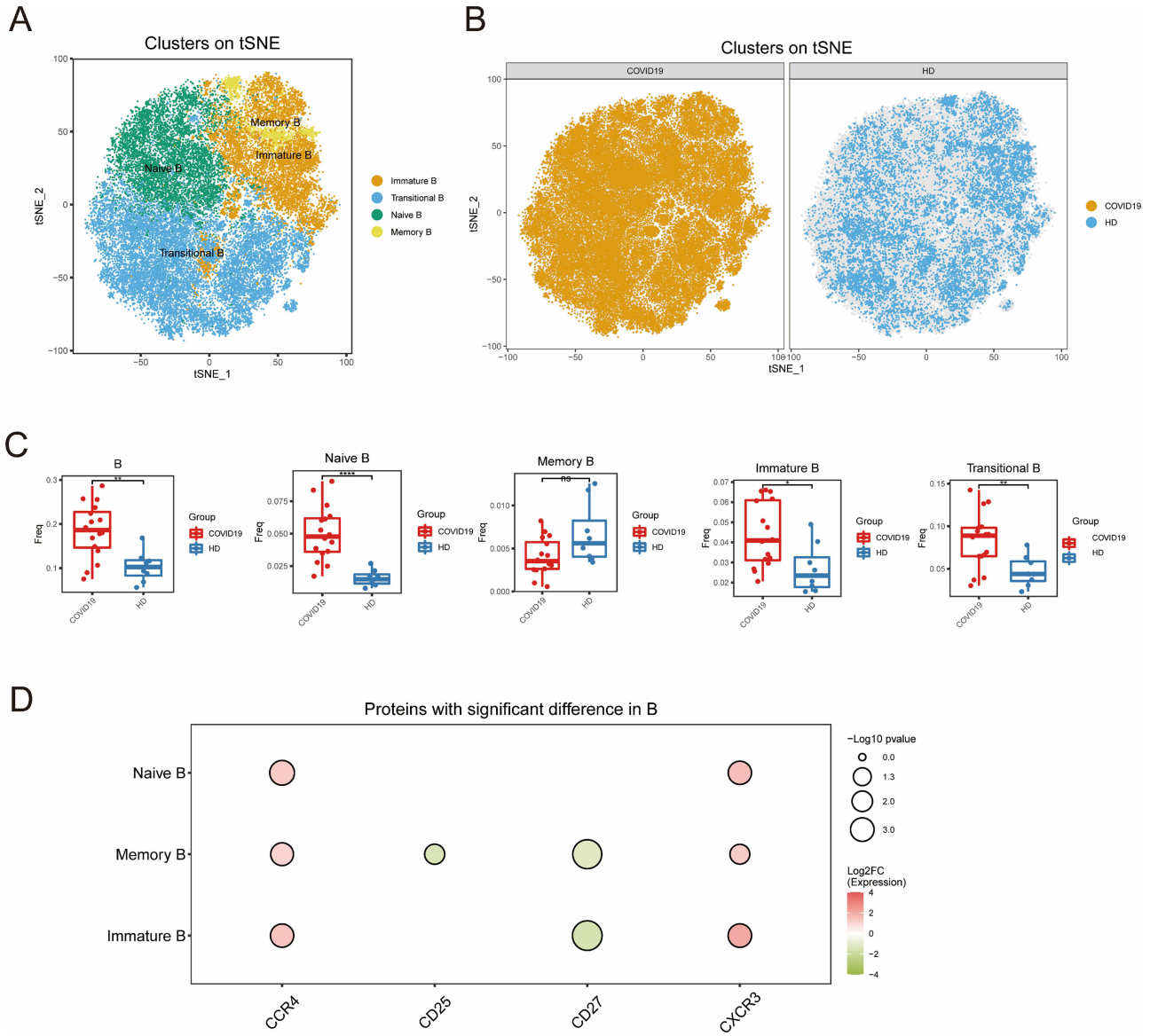

Figure 4 B-cell Subsets comparison in Healthy Donors and COVID-19 Patients. (**A**) t-Distributed Stochastic Neighbor Embedding (t-SNE) plot displaying the distribution of B-cell subsets, colored by cell type. (**B**) t-SNE projections illustrating major T-cell subsets in healthy donors and COVID-19 patients, colored by group. (**C**) Box plots depicting the frequency of B cells and their subtypes, which were significantly higher in covid-19 patients ($p<0.01$). (**D**) Bubble plots illustrating proteins with significant differential expression in B cell subtypes between groups. Dot size represents the negative log10 p-value, with green dots indicating higher expression in healthy donors and red dots indicating lower expression. Only proteins with an absolute log2 fold change over 1 and $p<0.05$ were selected for display following a unpaired Wilcoxon test. Significance levels were denoted as *P<0.05, **P<0.01, ***P<0.001, and ****P<0.0001.

higher levels of CCR4 and lower levels of CD44 and CD45 (Supplementary Figure 3A and B). An increased frequency in COVID19 of $CD4^{+}Foxp3^{+}CD33^{low}CD123^{+}CD38^{+}HLA\text{-}DR^{+}CXCR3^{+}$ plasmacytoid DCs (pDCs) was also observed, accompanied by elevated CD33 and decreased CXCR3 and CD123 expression (Supplementary Figure 3A and B). $CD56^{+}CD11c^{+}CCR4^{+}CXCR3^{+}Tbet^{+}$ NK cells had a higher frequency in COVID-19, with lower levels of CD16 and higher levels of CCR4, CD138, and CXCR3 (Supplementary Figure 3A and B).

Discussion

There have been studies utilizing high-throughput CyTOF technology to characterize SARS-CoV-2 specific immune cell responses.[15,20,21] Few studies have employed CyTOF to assess immune responses in pre-vaccinated patients. Our group is the first to utilize PBMCs from patients within one week after COVID-19 infection to evaluate immune responses in

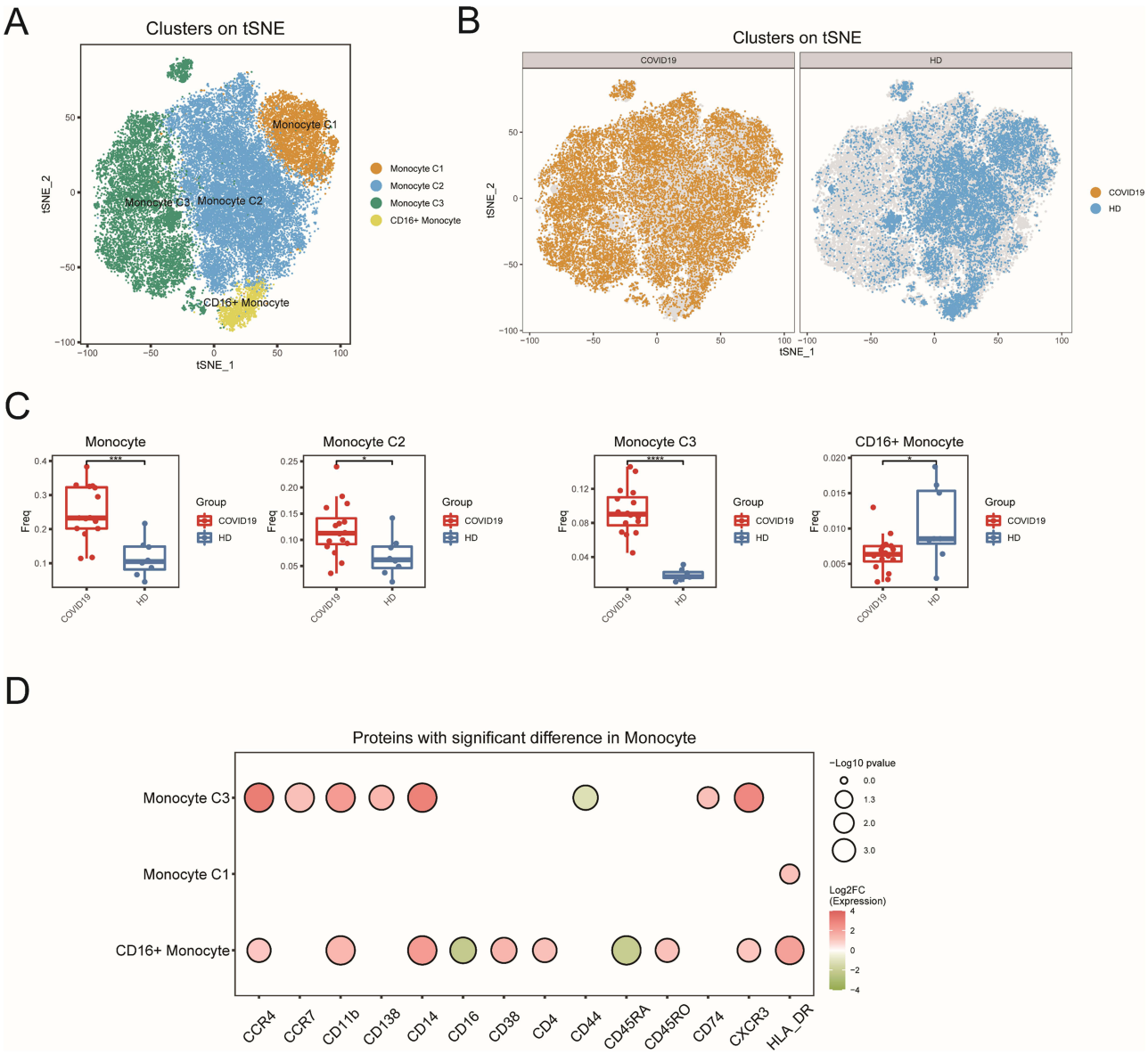

Figure 5 Monocyte cell Subsets comparison in Healthy Donors and COVID-19 Patients. (**A**) t-Distributed Stochastic Neighbor Embedding (t-SNE) plot displaying the distribution of Monocyte cell subsets, colored by cell type. (**B**) t-SNE projections illustrating major Monocyte cell subsets in healthy donors and COVID-19 patients, colored by group. (**C**) Box plots depicting the frequency of Monocyte cells and their subtypes, which were significantly higher in covid-19 patients ($p<0.01$). (**D**) Dot plots illustrating proteins with significant differential expression in B cell subtypes between groups. Dot size represents the negative log10 p-value, with green dots indicating higher expression in healthy donors and red dots indicating lower expression. Only proteins with an absolute log2 fold change over 1 and $p<0.05$ were selected for display following an unpaired Wilcoxon test. Significance levels were denoted as *P<0.05, **P<0.01, ***P<0.001, and ****P<0.0001.

ZF2001 vaccinated patients. Age is one of the risk factors for COVID-19.[22] All participants in this study were under 22 years old and had no comorbidities. Regarding the age of participants, only cancer was associated with higher odds of mortality.[23] Our study provided insight into the immune response to COVID-19 in healthy vaccinated adults. Although only three females participated as HD, male gender was linked to higher mortality rates in patients over 80.[23] Therefore, the findings from this study are still applicable to younger patients.

In contrast to COVID-19 patients without vaccination, the percentage of $CD8^+$ T effector cells increased to combat COVID-19 infections in this study.[15,24,25] Since only the proportion of CD4 cells decreased in the patient group, it is expected that the CD4/CD8 ratio would also drop in these patients. A higher CD4/CD8 ratio is associated with better outcomes for patients. One limitation of this study is that it only includes mild cases, so we do not know the CD4/CD8 ratio in more severe conditions. In unvaccinated scenarios, the proportions of Th1 and Th2 cells were diminished by COVID-19 infection.[26]

https://doi.org/10.2147/IDR.S511936

However, we did not observe a reduction in Th1 cells in our case, indicating a favourable role vaccination for patient's health. We did observe a decrease of CD27, CD272, and CD44 in subtypes of T cells which lower level of $CD4^+$ T cells differentiation and activation level.[27] CD44 is a multifunctional protein that facilitates cell-cell and cell-matrix interactions and acts as the primary signaling receptor for hyaluronan (HA).[28,29] In the context of COVID-19, interleukin-13 (IL-13) is thought to enhance HA synthesis, and the HA-CD44 interaction may recruit immune cells. However, in our study, we observed a decrease in CD44 across all identified T cell types.[28] This finding suggests that further research is needed to explore the role of CD44 in the immune response to viral infections following vaccination. We found that $Ki67^+CD8^+$ T effector cells express higher levels of PD-1 in COVID-19 patients, and some studies have reported upregulation of expression of inhibitory immune checkpoint receptors (eg, PD-1) and exhaustion-associated gene signatures in $CD8^+$ T cells from COVID-19 patients.[30–32] However, whether $CD8^+$ T cells are actually depleted during COVID-19 has been a controversial issue, and it has also been shown that $CD8^+$ T cells express PD-1, but that these cells are not depleted but are functional.[33,34] This suggests that in COVID-19 patients, PD-1 expression may reflect the activated state of T cells more than the depleted state. The expression of CXCR3 was elevated not only in T cells but also in all major cell types. CXCR3 plays a crucial role in the body's antiviral response, particularly in respiratory infections.[35] Our study demonstrated that vaccinated patients had a more active T cell response compared to unvaccinated patients.

According Çölkesen et al, to decrease of B lymphocytes, naïve B cells and switched memory B cells were in dependence risk factors for mortality in COVID-19 patients.[36] For COVID-19 patients who have never been infected or pre-vaccinated, the frequency of B cells was lower than HD.[37] Contrary to this, in our study, the frequency of B cells was significantly higher in the COVID-19 group, suggesting the efficacy of vaccination. Long-term immune protection is achieved through the induction of long-lived plasma cells and memory B cells. Our data illustrated that vaccinated patients had higher levels of plasma cells and memory B cells in response to COVID-19 compared to unvaccinated patients.[38,39] This provides evidence that ZF2001 vaccination is effective in promoting long-term immune protection. Due the limited space of antibodies in the panel, it was unable for us to separate double negative B cells from our research. According to a whom,[40] double negative B cells could be distributed in to DN2 ($CD21^-$ $CD11c^+$) and DN3 ($CD21^-$ $CD11c^-$) which correlates with more severe disease states. Especially DN3, lower oxygen saturation levels are associated with higher DN3. Further research is needed to fully understand the roles of DN2 and DN3 cells in health and disease, particularly in infectious processes like COVID-19.

We observe decreasing pattern of $CD16^+$ monocytes in COVID-19 groups which is contrary to unvaccinated study.[15,41] $CD16^+$ monocytes were considered as a negative factor of COVID19 patients due to its role in inflame response.[17] We have not found any research that describes the function of monocyte C1, C2 and C3 in COVID-19. The surface of C2 monocytes presents with CD272 and CD95. Although our research group is not the only one to detect CD272 on monocytes,[42,43] its function on these cells requires further research. However, since CD272 is co-expressed with CD95, which can lead to apoptosis,[44] it is reasonable to believe that C2 monocytes may be easily eliminated as part of immune regulation. In contrast, C3 monocytes express CCR4 and CXCR3, so they represent the primary source of inflammation in monocytes observed in our study. Research has been reported antigen-presenting function of DCs could be impaired by COVID-19 infection.[45] The situation in our study was complex. On one hand, the expression level of CD123 was decreased in COVID-19.[35] On the other hand, the frequency of pDCs was higher in COVID-19 patients. Therefore, the functional changes of pDCs induced by COVID-19 infection in vaccinated individuals still require further investigation. Myeloid-derived suppressor cells (MDSCs) comprise a diverse group of immune cells that are pivotal in mediating immunosuppression.[46] HLA-DR is commonly used as a negative marker for MDSCs. During our data analysis, we did not specifically target MDSCs for cell typing. However, we found that monocytes expressed higher levels of HLA-DR compared to healthy controls (HC), indicating a reduction in MDSCs within our patient group.

Our study also has some shortcomings and limitations. Our study has limitations in population size and requires follow-up at 1 year. In addition, CyTOF provides a great deal of detailed information about immune cell phenotypes and should be further utilized to study immune responses to other pathogens. And there are limitations to the cellular analysis that will require comparison of specific ratios of antibody subtypes (IgG1 and IgG3) in future kinetic studies.

Conclusions

In conclusion, our research using high-throughput CyTOF technology on ZF2001 vaccinated COVID-19 patients demonstrated distinct immune cell dynamics compared to unvaccinated individuals. Vaccinated patients maintained stable Th1 cell levels and exhibited an increased frequency of B cells, indicative of a robust antibody-mediated response. We observed altered T cell differentiation and activation patterns, with higher PD-1 expression on Ki67+CD8+ T effector cells suggesting activation. These findings highlight the effectiveness of ZF2001 in eliciting a comprehensive immune response, crucial for managing SARS-CoV-2 reinfection and supporting the ongoing use and development of COVID-19 vaccines.

Data Sharing Statement

All data generated or analyzed during this study are included in this article and its Supplementary Material files. Further enquiries can be directed to the corresponding author.

Ethics Statement

This study has been approved by the Medical Ethics Committee of Shijiazhuang No.5 hospital and the Medical Ethics Committee (Ethics Approval Number: 2022012). Written informed consents were obtained from each patient and healthy donors. In general, all data in this study were obtained in accordance with the Helsinki declaration.

Author Contributions

All authors made a significant contribution to the work reported, whether that is in the conception, study design, execution, acquisition of data, analysis and interpretation, or in all these areas; took part in drafting, revising or critically reviewing the article; gave final approval of the version to be published; have agreed on the journal to which the article has been submitted; and agree to be accountable for all aspects of the work.

Funding

This work was supported by the Shijiazhuang Technology Support Plan (231200243).

Disclosure

The authors report no conflicts of interest in this work.

References

1. Omotayo O, Muonde M, Olorunsogo TO, Ogugua JO, Maduka CP. Pandemic epidemiology: a comprehensive review of covid-19 lessons and future healthcare preparedness. *IMSRJ*. 2024;4(1):89–107. doi:10.51594/imsrj.v4i1.739
2. Liu J, Yu Y, Jian F, et al. Enhanced immune evasion of SARS-CoV-2 variants KP.3.1.1 and XEC through N-terminal domain mutations. *Lancet Infect Dis*. 2025;25(1):e6–e7. doi:10.1016/S1473-3099(24)00738-2
3. Brown B, Ojha V, Fricke I, et al. Innate and adaptive immunity during SARS-CoV-2 infection: biomolecular cellular markers and mechanisms. *Vaccines*. 2023;11(2):408. doi:10.3390/vaccines11020408
4. Al-Sheboul SA, Brown B, Shboul Y, Fricke I, Imarogbe C, Alzoubi KH. An immunological review of SARS-CoV-2 infection and vaccine serology: innate and adaptive responses to mRNA, adenovirus, inactivated and protein subunit vaccines. *Vaccines*. 2023;11(1):51. doi:10.3390/vaccines11010051
5. Krammer F. The role of vaccines in the COVID-19 pandemic: what have we learned? *Semin Immunopathol*. 2024;45(4–6):451–468. doi:10.1007/s00281-023-00996-2
6. House T, Riley H, Pellis L, et al. Inferring risks of coronavirus transmission from community household data. *Stat Methods Med Res*. 2022;31(9):1738–1756. doi:10.1177/09622802211055853
7. Patalon T, Gazit S, Pitzer VE, Prunas O, Warren JL, Weinberger DM. Odds of testing positive for SARS-CoV-2 following receipt of 3 vs 2 doses of the BNT162b2 mRNA vaccine. *JAMA Intern Med*. 2022;182(2):179–184. doi:10.1001/jamainternmed.2021.7382
8. Zhao X, Zheng A, Li D, et al. Neutralisation of ZF2001-elicited antisera to SARS-CoV-2 variants. *Lancet Microbe*. 2021;2(10):e494. doi:10.1016/S2666-5247(21)00217-2
9. Dai L, Gao L, Tao L, et al. Efficacy and safety of the RBD-dimer–based covid-19 vaccine ZF2001 in adults. *N Engl J Med*. 2022;386(22):2097–2111. doi:10.1056/NEJMoa2202261
10. Zhang Y, Fu Z, Zhang H, et al. Proteomic and cellular characterization of omicron breakthrough infections and a third homologous or heterologous boosting vaccination in a longitudinal cohort. *Mol Cell Proteomics*. 2024;23(6):100769. doi:10.1016/j.mcpro.2024.100769
11. Iyer A, Hamers AAJ, Pillai AB. CyTOF® for the Masses. *Front Immunol*. 2022;13:815828. doi:10.3389/fimmu.2022.815828
12. Han G, Spitzer MH, Bendall SC, Fantl WJ, Nolan GP. Metal-isotope-tagged monoclonal antibodies for high-dimensional mass cytometry. *Nat Protoc*. 2018;13(10):2121–2148. doi:10.1038/s41596-018-0016-7

13. Rubinstein A, Kudryavtsev I, Arsentieva N, Korobova ZR, Isakov D, Totolian AA. CXCR3-expressing T cells in infections and autoimmunity. *Front Biosci*. 2024;29(8):301. doi:10.31083/j.fbl2908301
14. Spoerl S, Kremer AN, Aigner M, et al. Upregulation of CCR4 in activated $CD8^+$ T cells indicates enhanced lung homing in patients with severe acute SARS-CoV-2 infection. *Eur J Immunol*. 2021;51(6):1436–1448. doi:10.1002/eji.202049135
15. Shi W, Liu X, Cao Q, et al. High-dimensional single-cell analysis reveals the immune characteristics of COVID-19. *Am J Physiol Lung Cell Mol Physiol*. 2021;320(1):L84–L98. doi:10.1152/ajplung.00355.2020
16. Hadjadj J, Yatim N, Barnabei L, et al. Impaired type I interferon activity and inflammatory responses in severe COVID-19 patients. *Science*. 2020;369(6504):718–724. doi:10.1126/science.abc6027
17. Merad M, Martin JC. Pathological inflammation in patients with COVID-19: a key role for monocytes and macrophages. *Nat Rev Immunol*. 2020;20(6):355–362. doi:10.1038/s41577-020-0331-4
18. Wang C, Xie J, Zhao L, et al. Alveolar macrophage dysfunction and cytokine storm in the pathogenesis of two severe COVID-19 patients. *EBioMedicine*. 2020;57:102833. doi:10.1016/j.ebiom.2020.102833
19. Wei P-F. Diagnosis and treatment protocol for novel coronavirus pneumonia (Trial Version 7). *Chinese Med J*. 2020;133(9):1087–1095. doi:10.1097/CM9.0000000000000819
20. Wang W, Su B, Pang L, et al. High-dimensional immune profiling by mass cytometry revealed immunosuppression and dysfunction of immunity in COVID-19 patients. *Cell Mol Immunol*. 2020;17(6):650–652. doi:10.1038/s41423-020-0447-2
21. Penttilä PA, Van Gassen S, Panovska D, et al.; The CONTAGIOUS consortium. High dimensional profiling identifies specific immune types along the recovery trajectories of critically ill COVID19 patients. *Cell Mol Life Sci*. 2021;78(8):3987–4002. doi:10.1007/s00018-021-03808-8
22. Liu K, Chen Y, Lin R, Han K. Clinical features of COVID-19 in elderly patients: a comparison with young and middle-aged patients. *J Infect*. 2020;80(6):e14–e18. doi:10.1016/j.jinf.2020.03.005
23. Zhang H, Wu Y, He Y, et al. Age-related risk factors and complications of patients with COVID-19: a population-based retrospective study. *Front Med*. 2022;8:757459. doi:10.3389/fmed.2021.757459
24. Odak I, Barros-Martins J, Bošnjak B, et al. Reappearance of effector T cells is associated with recovery from COVID-19. *EBioMedicine*. 2020;57:102885. doi:10.1016/j.ebiom.2020.102885
25. Wang L, Nicols A, Turtle L, et al. T cell immune memory after covid-19 and vaccination. *BMJ Med*. 2023;2(1):e000468. doi:10.1136/bmjmed-2022-000468
26. Gil-Etayo FJ, Suàrez-Fernández P, Cabrera-Marante O, et al. T-helper cell subset response is a determining factor in COVID-19 progression. *Front Cell Infect Microbiol*. 2021;11:624483. doi:10.3389/fcimb.2021.624483
27. Al-Zahrani MH, Alghamdi RA, Tarbiah NI, Alkhattabi NA, Joharjy HM, Khalifa RA. Role of CD27 and SAMHD1 and their genetic susceptibility to COVID-19. *Saudi J Biol Sci*. 2023;30(11):103821. doi:10.1016/j.sjbs.2023.103821
28. Albtoush N, Petrey AC. The role of hyaluronan synthesis and degradation in the critical respiratory illness COVID-19. *Am J Physiol Cell Physiol*. 2022;322(6):C1037–C1046. doi:10.1152/ajpcell.00071.2022
29. Baaten BJG, Li CR, Bradley LM. Multifaceted regulation of T cells by CD44. *Commun Integr Biol*. 2010;3(6):508–512. doi:10.4161/cib.3.6.13495
30. De Biasi S, Meschiari M, Gibellini L, et al. Marked T cell activation, senescence, exhaustion and skewing towards TH17 in patients with COVID-19 pneumonia. *Nat Commun*. 2020;11(1):3434. doi:10.1038/s41467-020-17292-4
31. Zheng HY, Zhang M, Yang CX, et al. Elevated exhaustion levels and reduced functional diversity of T cells in peripheral blood may predict severe progression in COVID-19 patients. *Cell Mol Immunol*. 2020;17(5):541–543. doi:10.1038/s41423-020-0401-3
32. Suryawanshi RK, Chen IP, Ma T, et al. Limited cross-variant immunity from SARS-CoV-2 Omicron without vaccination. *Nature*. 2022;607(7918):351–355. doi:10.1038/s41586-022-04865-0
33. Rha MS, Jeong HW, Ko JH, et al. PD-1-expressing SARS-CoV-2-specific CD8+ T cells are not exhausted, but functional in patients with COVID-19. *Immunity*. 2021;54(1):44–52.e3. doi:10.1016/j.immuni.2020.12.002
34. Rha MS, Shin EC. Activation or exhaustion of CD8+ T cells in patients with COVID-19. *Cell Mol Immunol*. 2021;18(10):2325–2333. doi:10.1038/s41423-021-00750-4
35. Liu K, Zhu M, Huang Y, Wei S, Xie J, Xiao Y. CD123 and its potential clinical application in leukemias. *Life Sci*. 2015;122:59–64. doi:10.1016/j.lfs.2014.10.013
36. Çölkesen F, Kurt EK, Vatansev H, et al. Memory B cells and serum immunoglobulins are associated with disease severity and mortality in patients with COVID-19. *Postgrad Med J*. 2022;98(1164):765–771. doi:10.1136/postgradmedj-2021-140540
37. De Biasi S, Lo Tartaro D, Meschiari M, et al. Expansion of plasmablasts and loss of memory B cells in peripheral blood from COVID-19 patients with pneumonia. *Eur J Immunol*. 2020;50(9):1283–1294. doi:10.1002/eji.202048838
38. Chen S, Guan F, Candotti F, et al. The role of B cells in COVID-19 infection and vaccination. *Front Immunol*. 2022;13:988536. doi:10.3389/fimmu.2022.988536
39. Ahmed N, Athavale A, Tripathi AH, et al. To be remembered: b cell memory response against SARS-CoV-2 and its variants in vaccinated and unvaccinated individuals. *Scandinavian J Immunol*. 2024;99(2):e13345. doi:10.1111/sji.13345
40. Sosa-Hernandez VA, Torres-Ruiz J, Cervantes-Diaz R, et al. B cell subsets as severity-associated signatures in COVID-19 patients. *Front Immunol*. 2020;11:611004. doi:10.3389/fimmu.2020.611004
41. Zheng Y, Liu X, Le W, et al. A human circulating immune cell landscape in aging and COVID-19. *Protein Cell*. 2020;11(10):740–770. doi:10.1007/s13238-020-00762-2
42. Li C, Xiao M, Geng S, et al. Comprehensive analysis of human monocyte subsets using full-spectrum flow cytometry and hierarchical marker clustering. *Front Immunol*. 2024;15:1405249. doi:10.3389/fimmu.2024.1405249
43. Lin D, Liu Q, Wang W, et al. Aberrant expression of miR-16, B12 and CD272 in peripheral blood mononuclear cells from patients with active tuberculosis. *Am J Transl Res*. 2020;12(10):6076.
44. Seyrek K, Espe J, Reiss E, Lavrik IN. The crosstalk of apoptotic and non-apoptotic signaling in CD95 system. *Cells*. 2024;13(21):1814. doi:10.3390/cells13211814
45. Winheim E, Rinke L, Lutz K, et al. Impaired function and delayed regeneration of dendritic cells in COVID-19. *PLoS Pathog*. 2021;17(10):e1009742. doi:10.1371/journal.ppat.1009742
46. Perfilyeva YV, Ostapchuk YO, Tleulieva R, et al. Myeloid-derived suppressor cells in COVID-19: a review. *Clin Immunol*. 2022;238:109024. doi:10.1016/j.clim.2022.109024

Infection and Drug Resistance

Dovepress
Taylor & Francis Group

Publish your work in this journal

Infection and Drug Resistance is an international, peer-reviewed open-access journal that focuses on the optimal treatment of infection (bacterial, fungal and viral) and the development and institution of preventive strategies to minimize the development and spread of resistance. The journal is specifically concerned with the epidemiology of antibiotic resistance and the mechanisms of resistance development and diffusion in both hospitals and the community. The manuscript management system is completely online and includes a very quick and fair peer-review system, which is all easy to use. Visit http://www.dovepress.com/testimonials.php to read real quotes from published authors.

Submit your manuscript here: https://www.dovepress.com/infection-and-drug-resistance-journal